Lethaia
AN INTERNATIONAL JOURNAL OF PALAEONTOLOGY AND STRATIGRAPHY

Chemotaxonomic comparison of the seed ferns *Odontopteris cantabrica* and *Odontopteris schlotheimii*, Middle Pennsylvanian Sydney Coalfield, Canada

JOSÉ A. D'ANGELO AND ERWIN L. ZODROW

LETHAIA

We present the first comparative spectrochemical data in the study history of *Odontopteris schlotheimii* Brongniart, 1828–1831 and *Odontopteris cantabrica* Wagner, 1969. These fossils co-occur in the shaley roof of the Lloyd Cove seam (Ro% = 0.65; Sydney Coalfield, Canada). Fourier transform-infrared spectra show that the sampled pinnules of both species are preserved as fossilized-cuticles. They are prominently aliphatic with distinct methylene and methyl peaks (at 2922 cm^{-1} and 2852 cm^{-1}); with relatively high contents of carbonyl groups (peaks at 1700 cm^{-1}) that indicate a high degree of molecular cross linking; and with smaller amounts of aromatics (peaks at 820 cm^{-1} and 750 cm^{-1}) with a low condensation degree of benzene rings. No differences among respective pinnules are inferred from the 3D chemometric model and associate significance tests by the analysis of variance ($\alpha = 0.05$). At the same time, this method provides new, chemical parameters that, in conjunction with morphological features, could be used to efficiently distinguish species. □ *Spectrochemistry*, Odontopteris schlotheimii, O. cantabrica, *chemotaxonomic comparison.*

José A. D'Angelo ✉ jose_dangelo@cbu.ca, Universidad Nacional de Cuyo, FCEN, M5502JMA, Mendoza, Argentina and Department of Mathematics, Physics and Geology, Cape Breton University, 1250 Grand Lake Rd., Sydney, Nova Scotia B1P 6L2, Canada; Erwin L. Zodrow [zzodrovii@gmail.com], 503 Coxheath Road, Sydney, Nova Scotia, Canada, B1R 1S1; *manuscript received on 30/10/2021; manuscript accepted on 04/02/2022; manuscript published on 07/09/2022 in* Lethaia 55(2).

The occurrence of *Odontopteris cantabrica* Wagner 1969 (in Wagner *et al.* 1969, p. 125) at the Lloyd Cove seam (Sydney Coalfield; Fig. 1) is used to introduce the 'Cantabrian Substage' in the phytostratigraphy of the North American Carboniferous System implying that the seam is lower Stephanian (Zodrow 1985, fig. 20; Zodrow & Cleal 1985). The species' identity is based on direct comparison with the pinnule morphology of the impression-preserved secondary pinnae of the type specimen from the lower Stephanian of the Cantabrian Mountains in Spain (cf. Zodrow 1985). Co-occurring at the Lloyd Cove seam is *Odontopteris schlotheimii* Brongniart, 1828–1831, identified by Zodrow with the support by M. Boersma, Utrecht (Zodrow 1985). Important to note is that compressions of *O. schlotheimii* from the type location at Manebach, Germany (upper Stephanian-Permian), are too highly coalified (Barthel & Amelang 2011, p. 16) to be suitable for spectrochemical comparison with the two odontopterid species of Sydney.

We report the first 3D chemometric odontopterid model and that the two odontopterid species from Sydney Coalfield are chemically indistinguishable in terms of types and relative contents of functional groups. This is premised not only on equal vitrinite reflectance values, e.g. Lafuente Diaz *et al.* (2021), but also on the same states of preservation (see Zodrow & D'Angelo 2019).

Materials and methods

The two studied species, preserved as fossilized-cuticles (Zodrow & Mastalerz 2001, 2009), originated from a 20–100 cm section of unaltered, shaley roof rock of the Lloyd Cove seam (Fig. 1 A–C; see also Zodrow 1985). The 0.65% vitrinite reflectance value of the seam corresponds to high volatile A bituminous coal (Zodrow *et al.* 2009, table 1; Grist *et al.* 1995; Hacquebard 1984) from which favourable ('mild') fossilizing conditions are inferred that permit meaningful chemical comparison between the two species (D'Angelo *et al.* 2012; Zodrow *et al.* 2009).

Pinnules of *O. schlotheimii* are obtained from a 7-cm-long specimen (Fig. 2A), with several attached complete ultimate pinnae that are assumed to represent the terminal portion of a bipartite frond above an ultimate dichotomy (see Zodrow 1985, text-Fig. 14). *Odontopteris cantabrica* pinnules are obtained from the largest known 22-cm specimen (Fig. 2C) with a

https://doi.org/10.18261/let.55.2.8

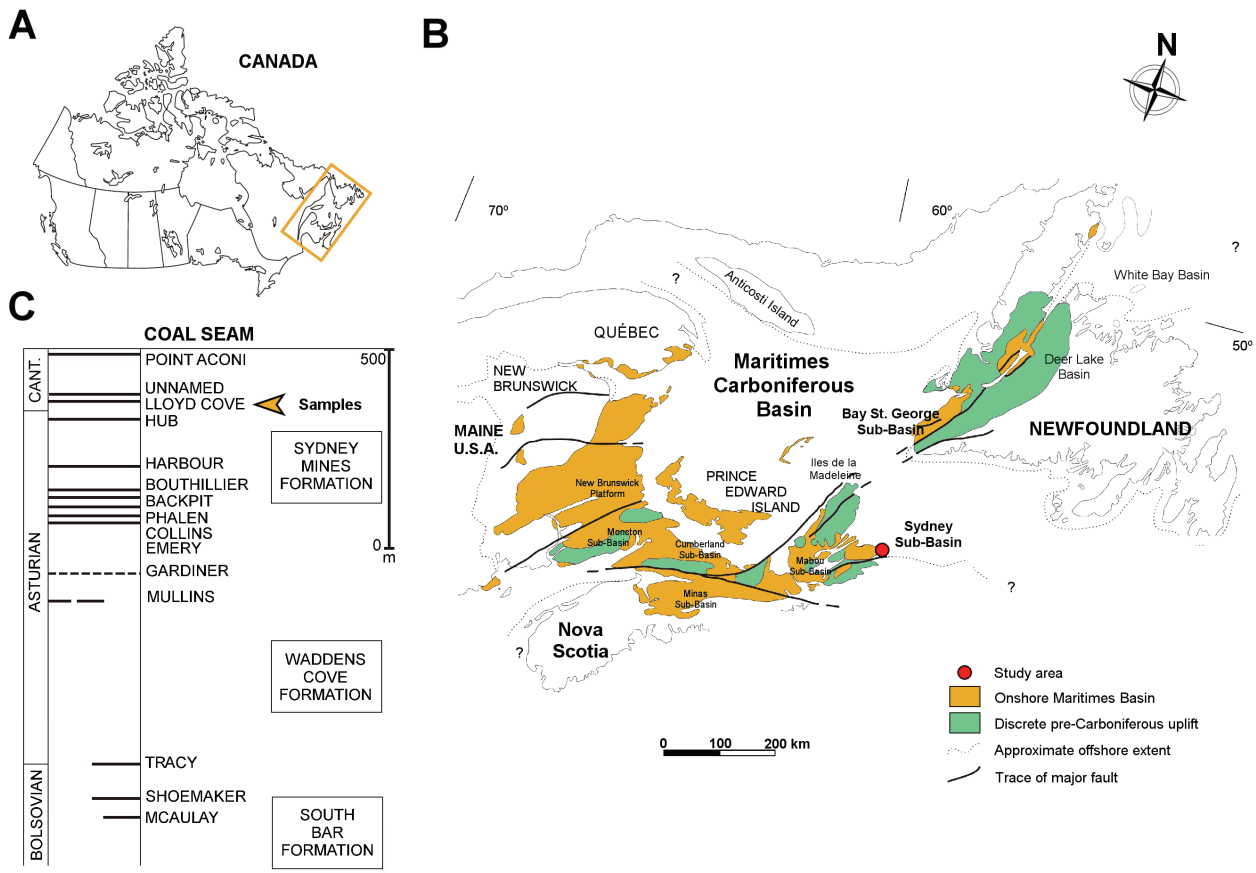

Fig. 1. Location map. A, Canada. B, Maritimes Basin with Sydney Coalfield (Sub-basin), Nova Scotia. C, lithostratigraphical column and sample location (arrowed) at the Lloyd Cove seam.

number of attached and complete ultimate pinnae. On macromorphological grounds, *O. schlotheimii* is distinguished from *O. cantabrica* by its long and linear terminal pinnules (Fig. 2A) as illustrated by Barthel & Amelang (2011, e.g. abb. 1a, 4, 4).

An arbitrary division into proximal and distal parts permitted more detailed chemometrical comparisons. In the case of the *O. schlotheimii* specimen, the distal pinnules include: S1 and S2; whereas the proximal part includes: S3, S4, S5, and S6. In the case of *O. cantabrica*, pinnules from the distal part include: C1, C2, C3, C4, and C5; whereas the proximal part includes: C6, C7, C8, C9, C10, and C11.

Coal (vitrain) samples from the Lloyd Cove seam are included in the analysis for comparative purposes.

Samples for the solid-state FTIR (Fourier transform infrared spectroscopy) are not chemically treated. They are prepared mixing powdered 0.5 mg to 2.0 mg of material (pinnules or vitrain) with 250 mg crystalline KBr. The mixture is ground, compressed into a pellet, and analyzed on a Nicolet Thermo-Electron 6700 spectrometer. Measurable conditions included 256 scans / spectrum at a resolution of 4 cm^{-1} wavenumber (details of the IR spectrometer characteristics and other measurement conditions can be found in Zodrow *et al.* 2009, p. 63). Noted is that, due to the small size of the pinnules, more than one (6–8) had to be used for obtaining the minimum sample amount mentioned above required to prepare KBr pellets.

Semi-quantitative FTIR analyses included the application of different processing techniques (i.e., Fourier self-deconvolution, areal integrative methods, and calculation of areal ratios) of the IR spectra (e.g. D'Angelo *et al.* 2010; Zodrow *et al.* 2009).

Results and discussion

Fourier transform infrared spectroscopy

Qualitative IR information: Both species show very similar IR spectra, exhibiting as a matter of fact, the same functional groups. Thus, only selected spectra are illustrated (Fig. 2B, D); however, peak assignments are applicable to all spectra.

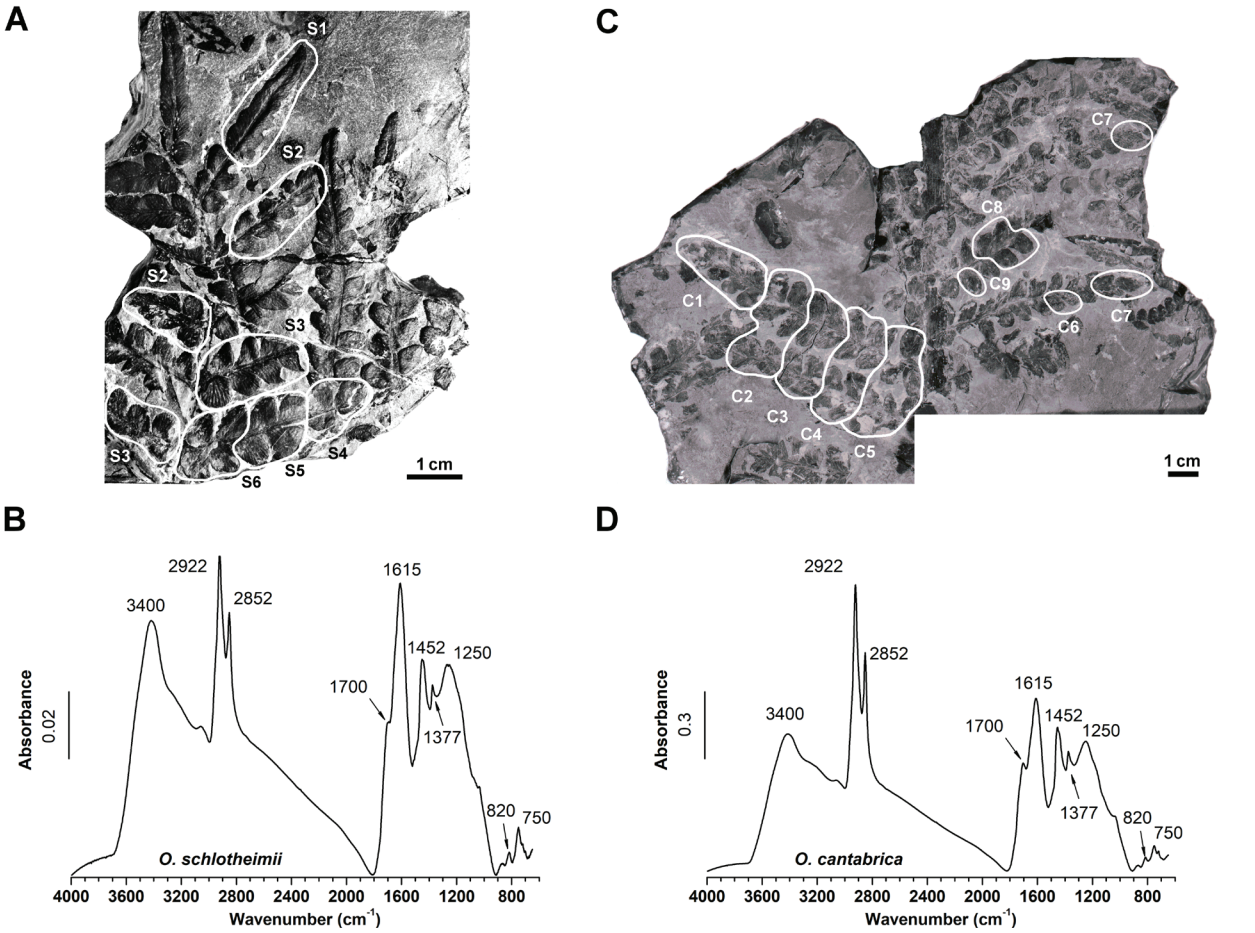

Fig. 2. Hand specimens and FTIR spectra. *Odontopteris schlotheimii*. A, specimen UCCB 981G-302a with approximate sample locations S1 – S6 (see Zodrow 1985, pl. 2). B, selected FTIR spectrum. *Odontopteris cantabrica*. C, specimen 981GF-458-0 with approximate sample locations C1 – C9 (see Zodrow 1985; Pl. 1). D, selected FTIR spectrum. The study material is on deposit with the Palaeobotanical Fossil Collection of Cape Breton University, Sydney, Nova Scotia, Canada.

A relatively broad and intense band centered at 3400 cm^{-1} is attributed to the H-bonded hydroxyl stretch, and the small peaks at 3050 cm^{-1} to aromatic C-H out-of-plane stretching vibrations. Prominent peaks assigned to aliphatic C-H stretching are centered at 2922 cm^{-1} and 2852 cm^{-1}, and carbonyl groups (possible ketones and carboxylic acids) are represented by the small peak at 1700 cm^{-1} (which are barely detectable in the coal samples). Peaks at 1600 cm^{-1} – 1615 cm^{-1} are ascribed to the C=C stretching of aromatic-carbon groups, and peaks at 1452 cm^{-1} to C-H alky-bending deformations. Noted is that the 1220 cm^{-1} – 1250 cm^{-1} band could be assigned to C-O stretching in both phenoxy and aromatic-ether structures. Small peaks at 820 cm^{-1} and 750 cm^{-1} are assigned to aromatic C-H out-of-plane bending vibrations, which have been ascribed to the contribution of vitrinitic matter (Lyons *et al*. 1995; Zodrow & Mastalerz 2002).

IR-derived data, definitions of semi-quantitative, and areal ratios derived from FTIR spectra are given by Table 1.

Both species show relatively high values of the methylene / methyl (CH_2/CH_3) ratio, carbonyl / aromatic carbon (C=O/C=C) group ratios, and the 'A' factor (Table 2), as well as relatively low values of aromatic carbon contribution (C=C cont).

Coal (vitrain) exhibits the highest contents of aromatics as is evident from the high values of C=C cont (Table 2).

The following sections describe detailed functional-group comparisons among samples, using multivariate analysis (a chemometric approach) of the four semi-quantitative IR-derived ratios, i.e., CH_2/CH_3, 'A' factor, and C=O/C=C, and C=C cont.

3D Multivariate Model

Three principal components (PCs) account for 98.9% cumulative variance (Tables 1–3, Appendix; supplementary data). The plots of component loadings and component scores are shown in Figure 3 (A, B, D, E).

Table 1. Definition of area ratios derived from FTIR spectra. Further details can be found in D'Angelo *et al.* (2010, 2012)

Ratio	Band-region (cm^{-1})	Interpretation and remarks
	Band-region ratios	
CH_2/CH_3	3000–2800	Methylene/methyl ratio. It relates to aliphatic chain length and degree of branching of aliphatic side groups (side chains attached to macromolecular structure; Lin & Ritz, 1993a, b). Higher value implies comparatively longer and straight chains, a lower value shorter and more branched chains. Caution is advised using the ratio, as it may be misleading due to the contribution from CH_2 and CH_3 groups attached directly to aromatic rings (Petersen & Nytoft, 2006).
C=O/C=C	(1700–1600) / (1600–1500)	Carbonyl/aromatic carbon groups ratio. Relative contribution of carbonyl (C=O) to aromatic carbon (C=C) groups. Higher values indicate increasing carbonyl/carboxyl groups to aromatic carbon groups (Mastalerz & Bustin, 1997).
C=C cont	(~1600) / (1800–1600)	Aromatic carbon contribution. Relative contribution of aromatic carbon groups (C=C; peak in 1650 to 1520 cm^{-1} region, centered near 1600 cm^{-1}) to combined contribution of oxygen-containing groups and aromatic carbon (C=C) structures (Mastalerz & Bustin, 1997).
'A' factor = $CH_{al}/(CH_{al}$ + C=C)	(3000–2800) / [(3000–2800) + (1650–1520)]	Relative contribution of aliphatic C-H stretching bands (CH_{al}) to sum of aliphatic C-H stretching and aromatic carbon structures. According to Ganz & Kalkreuth (1987) it represents change in relative intensity of aliphatic groups.

Table 2. Semi-quantitative FTIR data set obtained for pinnules of *Odontopteris cantabrica* and *O. schlotheimii* from the Lloyd Cove seam, Sydney Coalfield, Nova Scotia, Canada

#	Taxon/sample	Sample form[a]	ID	CH_2/CH_3	C=O/C=C	C=C cont	'A' factor
1	*O. cantabrica*	FC	**C1**	3.8	0.3	0.23	0.8
2	*O. cantabrica*	FC	**C2**	3.6	0.2	0.26	0.8
3	*O. cantabrica*	FC	**C3**	3.4	0.2	0.24	0.73
4	*O. cantabrica*	FC	**C4**	3.4	0.2	0.19	0.79
5	*O. cantabrica*	FC	**C5**	3.4	0.09	0.27	0.8
6	*O. cantabrica*	FC	**C6** [b]	4.7	0.1	0.28	0.69
7	*O. cantabrica*	FC	**C7** [b]	4.1	0.09	0.34	0.78
8	*O. cantabrica*	FC	**C8** [b]	4.7	0.1	0.26	0.73
9	*O. cantabrica*	FC	**C9** [b]	3.1	0.06	0.45	0.55
10	*O. cantabrica*	FC	**C10**	3.4	0.08	0.26	0.78
11	*O. cantabrica*	FC	**C11**	3.7	0.07	0.36	0.75
12	*O. schlotheimii*	FC	**S1**	4.6	0.2	0.24	0.74
13	*O. schlotheimii*	FC	**S2**	4	0.2	0.24	0.74
14	*O. schlotheimii*	FC	**S3**	3.4	0.1	0.28	0.69
15	*O. schlotheimii*	FC	**S4**	3	0.09	0.31	0.74
16	*O. schlotheimii*	FC	**S5**	3.6	0.08	0.35	0.7
17	*O. schlotheimii*	FC	**S6**	5	0.07	0.3	0.75
18	Coal	Vitrain	**V** [c]	0.9	0.003	0.77	0.41
19	Coal	Vitrain	**V** [c]	0.8	0.03	0.74	0.35
20	Coal	Vitrain	**V** [c]	1	0.007	0.64	0.4

[a] Sample form: FC = fossilized cuticle.
[b] Taken from Zodrow et al. (2012).
[c] Taken from D'Angelo et al. (2010).

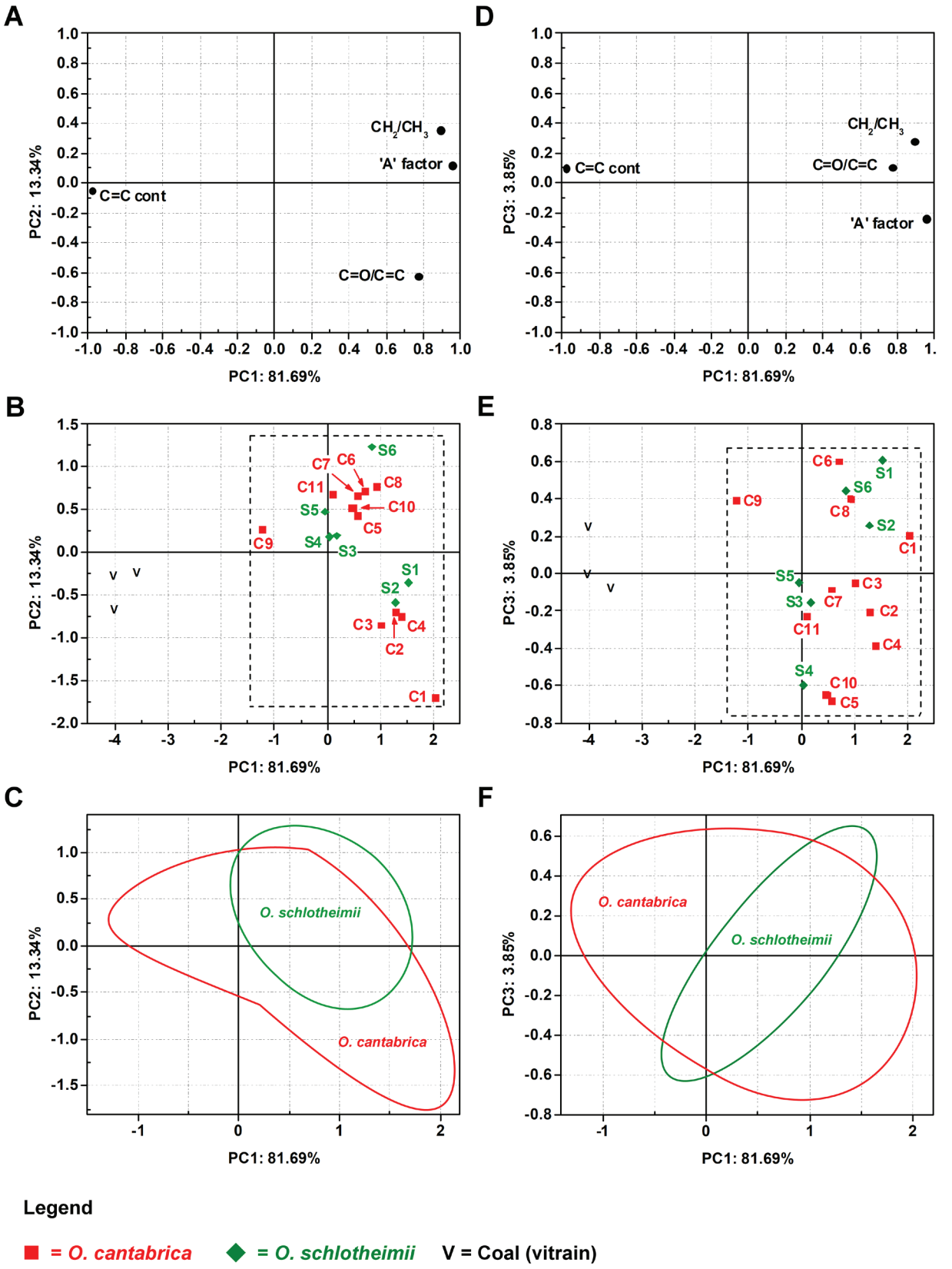

Fig. 3. Principal component analysis (PCA). A, plot of PC 1 vs. PC 2 component loadings. B, plot of PC 1 vs. PC 2 component scores. C, simplified plot of the area delimited in B showing data groupings corresponding to *O. schlotheimii* and *O. cantabrica*. D, plot of PC 1 vs. PC 3 component loadings. E, plot of PC 1 vs. PC 3 component scores. F, simplified plot of the area delimited in E showing the two species. Delimiting ellipses around the groups have no statistical significance.

PC 1 (81.69% explained variance) has high positive loadings on CH_2/CH_3, 'A' factor, and C=O/C=C, and a high negative loading on C=C cont (Fig. 3A). This pattern reflects the abundance of longer and poorly branched, polymethylenic [$(-CH_2-)_n$] side chains containing oxygen-bearing compounds vs. aromatic groups (Table 2).

Most of the samples (i.e. C1 – C8, C10, C11, S1 – S4, and S6) exhibit positive scores against PC 1 (Fig. 3B, *x* axis). This is related to the medium to high contents of aliphatic compounds with longer and relatively straight hydrocarbon chains. Vitrain samples, as well as C9 and S5, have negative scores against PC 1 (Fig. 3B, *x* axis), because of their medium to high values of C=C cont (Table 2).

PC 2 (13.34% explained variance) has a high negative loading on the C=O/C=C ratio indicating the abundance of carbonyl-bearing functionalities (Fig. 3B). Implied are higher C=O contents and the likely presence of ester bridges that form crosslinked bonds connecting one monomer chain to another one.

Distal C1 – C5 and distal S1 – S2, have medium to high C=O/C=C values (Fig. 3B, *y* axis). On the other hand, proximal C6 – C11 and proximal S3 – S6, have intermediate to low values of the C=O/C=C ratio. Proximal C9 exhibits a positive score against PC 2 mainly due to its very high C=C cont and the low C=O/C=C value, which is probably explained by the lower natural-maceration degree of this sample.

PC 3 (3.85% explained variance) has a low positive loading on the CH_2/CH_3 ratio, as well as a low negative loading on the 'A' factor (Fig. 3D). Samples C1, C6, C8, C9, S1, S2, and S6 have positive scores against PC 3 (Fig. 3E, *y* axis), as a consequence of their medium

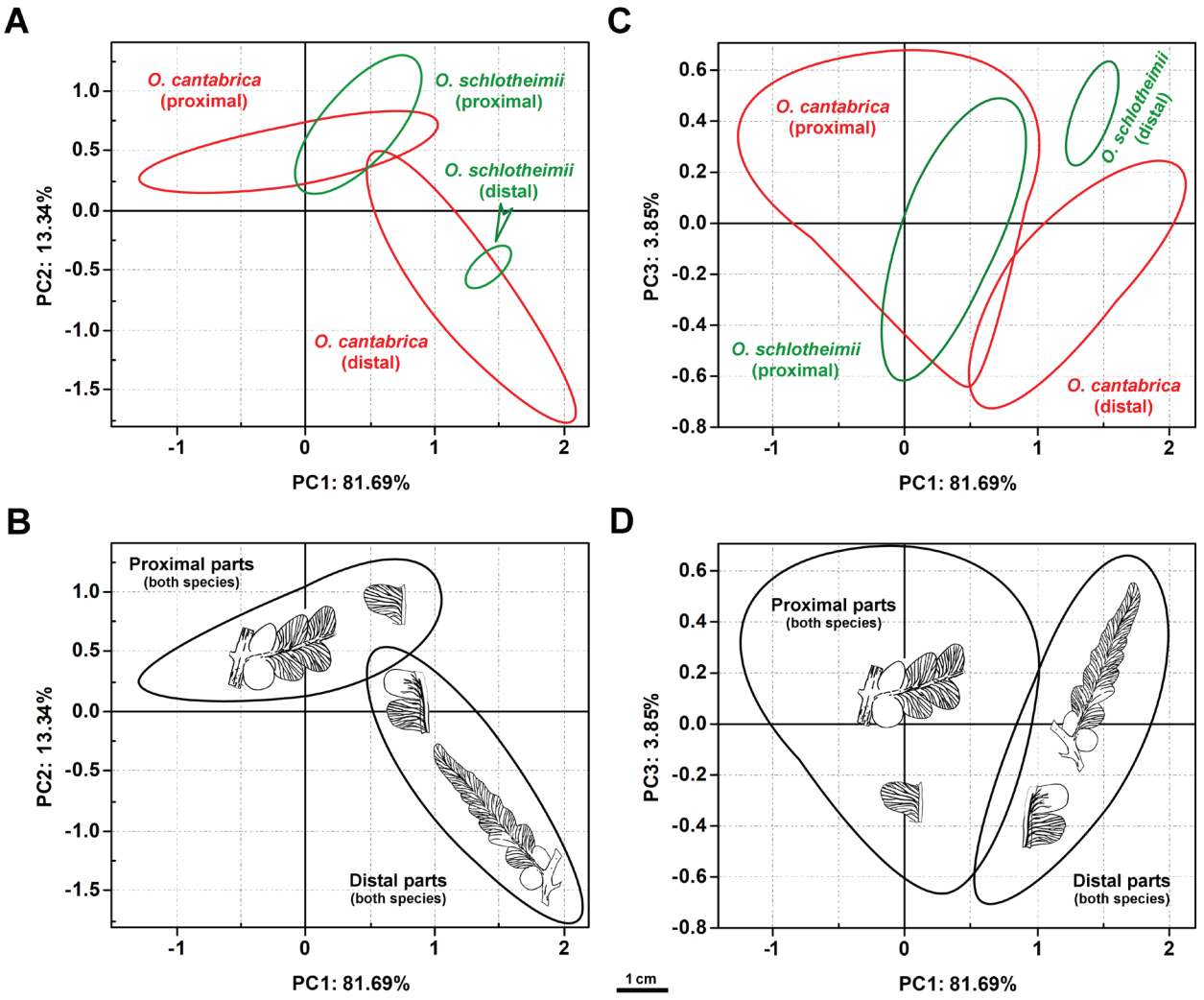

Fig. 4. A, B, simplified plots of the areas delimited in Figure 3B and E, respectively. Data groupings indicate the approximate component-plane zones corresponding to proximal and distal locations of pinnules. Notably, proximal and distal pinnules each overlap, but distal pinnules of the two species are separated (C and D). Elliptical zones are for clarity only. See text for details.

values of CH_2/CH_3 (Table 2). All the other samples (C2, C3, C4, C5, C7, C10, C11, S3, S4, and S5) have negative scores against PC 3 because of their relatively low values of the CH_2/CH_3 ratio, indicating their relatively shorter and more branched polymethylenic chains. Noted is that sample C9 has one of the highest positive scores against PC 3 as a consequence of its 'A' factor value, which is the lowest of the entire data set of pinnules. This is additional evidence supporting the lowest degree of natural maceration (the lowest aliphatic content = the lowest 'A' factor value) of sample C9.

Chemotaxonomic comparison

Simplified plots (Fig. 3C and F) exhibit the groupings of samples corresponding to *O. schlotheimii* and *O. cantabrica* which are indicated by delimiting ellipses around the groups (having no statistical significance).

Principal components retained (i.e., PC 1, PC 2, and PC 3; linear combinations of the original variables = chemical functionalities) account for 98.9% cumulative variance (see Tables 1–3, Appendix; supplementary data). These three PCs could be considered reliable proxies for the samples' chemical composition. Although the total number of studied samples is relatively small, and with *caveats*, one-way ANOVA tests of the PCA model can be performed. With 95% confidence, the PCs cannot be statistically differentiated ($p > 0.05$, Table 4, Appendix; supplementary data).

A more detailed examination of data plotted in Figure 3 (B, E) indicates that for each species a further distinction can be made among the PC data that represent proximal and distal pinnules. This is shown by simplified score plots (Fig. 4A, B, C, and D; ellipses are for clarity only) that reflect the main chemical characteristics of the proximal and distal pinnules of the two specimens (see the ANOVA test in Table 5, Appendix; supplementary data).

As inferred from the ANOVA tests: 1, proximal-pinnule groups of both species are not significantly different (Fig. 4A, C; Table 6, Appendix; supplementary data); 2, distal-pinnule groups cannot be differentiated either (Fig. 4B, D; Table 6, Appendix; supplementary data); and 3, proximal-pinnule groups of both species are significantly different from distal-pinnule groups of both species (Fig. 4B, D; Table 7, Appendix; supplementary data).

Conclusions

On macromorphological grounds *O. schlotheimii* and *O. cantabrica* are distinguishable from one another in the Sydney Coalfield, Canada. However, inferred from the IR-based PCA model and statistical significance tests (ANOVA, $\alpha = 0.05$) is that they are chemically indistinguishable when considering type and relative contents of functional groups. Stressed are common preservation states as fossilized cuticles at a low coal rank (0.65% vitrinite reflectance) as prerequisites for meaningful chemometrical comparison. In a future paper, together with newly discovered micromorphological features of *Odontopteris schlotheimii*, taxonomic, and biostratigraphical consequences of the inference of no chemical distinction will be presented.

Acknowledgements. – We are indebted to J. MacInnis (Molecular Spectroscopy Research Laboratory), Cape Breton University, for the use of the FTIR facilities to obtain the infrared spectra, G. M. Del Fueyo (Museo Argentino de Ciencias Naturales 'Bernardino Rivadavia', Buenos Aires) for thoughtful technical suggestions, and T. M. Zodrow (British Columbia) for editorial assistance. We gratefully acknowledge the suggestions and comments by the anonymous journal reviewer that improved style and technical content of this contribution.

References

Barthel, M., & Amelang, A., 2011. Der Farnsamer *Odontopteris schlotheimii* Brongniart aus der Manebach-Formation des Thüringer Wald-Beckens. *Semana 26*, 13–24.

Brongniart, A., 1828–1831. *Histoire des végétaux fossiles, ou recherché botaniques et géologiques sur les végétaux renfermés dans les diverses couches du globe*. Dufour et d', Paris. Ocagne p. 256, pl. LXXVIII, fig. 5.

D'Angelo, J.A., Zodrow, E.L., & Camargo, A., 2010. Chemometric study of functional groups in Pennsylvanian gymnosperm plant organs (Sydney Coalfield, Canada): implications for chemotaxonomy and assessment of kerogen formation. *Organic Geochemistry 41*, 1312–1325.

D'Angelo, J.A., Zodrow, E.L., & Mastalerz, M., 2012. Compression map, functional groups and fossilization: a chemometric approach (Pennsylvanian neuropteroid foliage, Canada). *International Journal of Coal Geology 90*, 149–155.

Ganz, H., & Kalkreuth, W., 1987. Application of infrared spectroscopy to the classification of kerogen-types and the evolution of source rock and oil–shale potentials. *Fuel 66*, 708–711.

Grist, A.M., Ryan, R.J., & Zentilli, M., 1995. The thermal evolution and timing of hydrocarbon generation in the Maritimes Basin of eastern Canada: evidence from apatite track data. *Canadian Society of Petrology and Geology Bulletin 43*, 145–155.

Hacquebard, P.A., 1984. Coal rank changes in the Sydney and Pictou Coalfields of Nova Scotia; cause and economic significance. *CIM Bulletin 77*, 33–40.

Lafuente Diaz, M.A., Del Fueyo, G.M., D'Angelo, J.A., & Carrizo, M.A., 2021. How much does Chemotaxonomy help to resolve the overrepresented *Cycadolepis* Saporta (Bennettitales)? A case study of the Cretaceous of Patagonia, Argentina. *Review of Palaeobotany and Palynology 293*, 104489.

Lin, R., & Ritz, G.P., 1993a. Reflectance FT-IR microspectroscopy of fossil algae contained in organic-rich shale. *Applied Spectroscopy 47*, 265–271.

Lin, R., & Ritz, G.P., 1993b. Studying individual macerals using i.r. microspectroscopy, and implications on oil versus gas/condensate proneness and 'low-rank' generation. *Organic Geochemistry 20*, 695–706.

Lyons, P.C., Orem, W.H., Mastalerz, M., Zodrow, E.L., Vieth-Redemann, A., & Bustin, R.M., 1995. ^{13}C NMR, micro-FTIR, and fluorescence spectra, and pyrolysis-gas chromatograms of coalified foliage of late Carboniferous medullosan seed

ferns, Nova Scotia, Canada: implications for coalification and chemotaxonomy. *International Journal of Coal Geology 27*, 227–248.

Mastalerz, M., & Bustin, R.M., 1997. Variation in chemistry of macerals in coals of the Mist Mountain Formation, Elk Valley coalfield, British Columbia, Canada. *International Journal of Coal Geology 33*, 43–59.

Petersen, H.I., & Nytoft, H.P., 2006. Oil generation capacity of coals as a function of coal age and aliphatic structure. *Organic Geochemistry 37*, 558–583.

Wagner, R.H., 1969. 4. Palaeontological Notes: fossil floras, p. 125–127. *In* Wagner, R.H., Villegas, F.J. & Fonolia, F. 1969. Description of the Lower Cantabrian Stratotype near Tejerina (León, N.W. Spain). *C.R. 6e Congress International Stratigraphy. Carboniferous*, Sheffield 1967, 115–138.

Zodrow, E.L., 1985. *Odontopteris* Brongniart in the Upper Carboniferous of Canada. *Palaeontographica Abteilung B 196*, 79–110.

Zodrow, E.L., & Cleal, C.J. 1985. Phyto- and chronostratigraphical correlation between the late Pennsylvanian Morien Group (Sydney, Nova Scotia) and the Silesian Pennant Measures (south Wales). *Canadian Journal of Earth Sciences 22*, 1465–1473.

Zodrow, E.L., & D'Angelo, J.A., 2019. Chemometric-based, 3D chemical-architectural model of *Odontopteris cantabrica* Wagner (Medullosales, Pennsylvanian, Canada): Implications for natural classification and taxonomy. *International Journal of Coal Geology 207*, 12–25.

Zodrow, E.L., & Mastalerz, M., 2001. Chemotaxonomy for naturally macerated tree-fern cuticles (Medullosales and Marattiales), Carboniferous Sydney and Mabou Sub-Basins, Nova Scotia, Canada. *International Journal of Coal Geology 47*, 255–275.

Zodrow, E.L., & Mastalerz, M., 2002. FTIR and py-GC–MS spectra of true-fern and seed-fern sphenopterids (Sydney Coalfield, Nova Scotia, Canada, Pennsylvanian). *International Journal of Coal Geology 51*, 111–127.

Zodrow, E.L., & Mastalerz, M., 2009. A proposed origin for fossilized Pennsylvanian plant cuticles by pyrite oxidation (Sydney Coalfield, Nova Scotia, Canada). *Bulletin of Geosciences 84*, 227–240.

Zodrow, E.L., D'Angelo, J.A., Mastalerz, M., & Keefe, D., 2009. Compression-cuticle of seed ferns: Insights from liquid-solid states FTIR (Late Palaeozoic-Early Mesozoic, Canada-Spain-Argentina). *International Journal of Coal Geology 79*, 61–73.

Zodrow, E.L., D'Angelo, J.A., Helleur, R., & Šimůnek, Z., 2012. Functional groups and common pyrolysate products of *Odontopteris cantabrica* (index fossil for the Cantabrian Substage, Carboniferous). *International Journal of Coal Geology 100*, 40–50.